Observation of water transport in the micro-porous layer of a PEFC with a freezing method and cryo-SEM

Yusuke Aoyama*, Kengo Suzuki, Yutaka Tabe, Takemi Chikahisa
Division of Energy and Environmental Systems, Graduate School of Engineering, Hokkaido University
N13 W8, Kita-ku, Sapporo, Hokkaido, 060-8628, Japan

* Corresponding author. Tel.: +81 11 706 6334; fax: +81 11 706 7889.
E-mail address: y.aoyama@eng.hokudai.ac.jp (Y. Aoyama).

ABSTRACT

Micro-porous layers (MPLs) play an important role in the water management of polymer electrolyte fuel cells (PEFCs), however, the detailed mechanism of how the produced water is drained from these layers is not well understood. This paper observed the cross-sectional distribution of liquid water inside the cathode MPL to elucidate details of the phase state of the water transported through the MPL. The freezing method and cryo-scanning electron microscope (cryo-SEM) are used for the observations; the freezing method enables immobilization of the liquid water in the cell as ice forms by the freezing, and the cryo-SEM can visualize the water distribution in the vicinity of the MPL at high resolution without the ice melting. It was shown that no liquid water accumulates inside the MPL in operation at 35ºC, while the pores of the MPL are filled with liquid water under very low cell temperature operation, at 5ºC. These results indicate that the produced water passes through the MPL not as a liquid but in the vapor state in usual PEFC operation. Additionally, liquid water at the interface between the MPL and a catalyst layer (CL) was identified, and the effect of the interfacial contact on the water distribution was examined.

Keywords: PEFC, MPL, Direct observation, Water transport, Phase state

1. Introduction

The PEFC is a promising power device in many fields, but some issues remain to be resolved before practical use can be realized. One important issue is water flooding where the accumulation of surplus produced water causes serious deterioration of the cell performance. The MPL is an important component in the water management as it suppresses flooding, as has been widely reported [1−8], however, the actual mechanism of this flooding suppressing role is not fully understood. Especially, details of the phase of the produced water in MPLs are not fully understood [3−8]. It is of vital significance to obtain accurate details of the phase state of the produced water to be able to understand the role of the MPL in the water transport.

The visualization of the actual liquid water transported through the MPL would be required to establish the phase state of the transported water, and there are few studies focusing on the visualization of the water transport in the MPL. The visualization methods for the water transfer phenomena in a membrane electrode assembly (MEA) commonly used in published studies have been neutron radiography and X-ray radiography [9−11]. Sasabe et al. visualized the liquid water flow in a crack in the MPL from the CL to the gas diffusion layer (GDL) by using a soft X-ray radiography technique and a specially designed infinitely-thin

cell [11]. However, the visualization of the liquid water with higher spatial resolutions using a cell with a commonly-used structure is needed to be able to specify the phase state of the water transported through the MPL, because the pore scale of the MPL is much smaller than the crack and the water transport is strongly affected by the temperature distribution in the vicinity of the MPL.

This study proposes a new observation method, which is termed the freezing method in this paper. Because the freezing method immobilizes liquid water as ice which can be directly observed, this method can be applied to various types of cells. Further, by using cryo-SEM as the observation apparatus, it becomes possible to visualize water transport in the MPL at high resolutions, maintaining the ice without melting. By this observation method, the cross-sectional distribution of liquid water inside the cathode MPL was investigated to elucidate the phase state of the water in MPLs. In addition, the differences in water distribution in two places were also examined, under gas-flow channels and at lands, both inside the MPL and at the interface between the MPL and CL.

2. Experimental apparatus and method

The single cell used in this study was composed of an MEA manufactured by GORE-TEX (PRIMEA® 5570/CNW20B, 0.4mg/cm^2 Pt loadings, 233μm thick GDLs with MPL), and the active area of the MEA was 1.8cm^2 (0.9cm × 2.0cm). Both the anode and cathode side bipolar plates had straight flow channels, the widths of the channels and lands were 1.0mm, and the channel height was 0.5mm. Hydrogen and air were used for the anode and cathode gases, respectively. In the experiments, the cell was set in a thermostatic chamber to keep the cell temperature constant.

Figure 1 shows the procedures of the freezing method. The method immobilizes the liquid water as ice by rapidly freezing the cell immediately after discontinuing operation. The freezing method consists of the steps detailed next. First, after shutting off the cell, it is rapidly cooled in a thermostatic chamber to secure the liquid water where it is at the instant of the shutdown. The authors have confirmed the water moved little during the cooling process in a limited experiment [12]. Next, the MEA is extracted from the cell, and immediately immersed in liquefied nitrogen to prevent sublimation of the frozen water by the further cooling. Then, the MEA is cut into several pieces, set in the sample holder, and moved to the vacuum chamber at –150°C in the cryo-SEM. Now the sample is cut by a cold knife, and the cut surface of the sample was coated with Au–Pd for clear observations. Finally, the sample can be observed by the cryo-SEM with an acceleration voltage of 5kV.

After the observations the temperature is raised to allow sublimation of the ice, and the ice can be discriminated by comparing the cryo-SEM images taken before and after the ice sublimates. Figure 2 shows an example where (a) and (b) are the cryo-SEM images before and after the sublimation at the same observation point, in Case B which will be shown later. Comparing the two photos, the layer between the MPL and the catalyst coated membrane (CCM) has vanished after the sublimation.

In this study, two operating conditions, Case A and Case B, were selected for the investigation of the state of the produced water passing through the cathode MPL. The cell temperatures of Cases A and B were set at 35ºC and 5ºC respectively. Here, Case B is much lower than normal operating conditions, and it becomes possible to analyze the relation

between water transport behavior and temperatures. In the two cases the same current density and gas flow rate were applied: the current density was 0.7A/cm^2, and the gas flow rates were 100sccm (standard cc/min = 1.67 x 10^{-8}m^3/s) for the anode hydrogen and 400sccm for the cathode air. The relative humidity of the supplied gases in Case A was 100%, and dry gas was supplied in Case B.

3. Results and discussion

Figure 3 shows the changes in the cell voltage and resistance for Cases A (35ºC) and B (5ºC). The cell voltage with Case B is lower than that with Case A, suggesting that much of the produced water condenses and that water flooding may occur in Case B. The higher cell resistance with Case B is due to the temperature dependence of the membrane: the resistance of the membrane increases as the temperature decreases.

Figure 4 shows cryo-SEM images of the cross-section of the MEA in the vicinity of the cathode MPL. Figures 4(a) and (b) are images taken before operating the cell; Fig. 4(a) is of the inside of the MPL, and (b) is at the MPL/CL interface. Before the cell operation, a porous structure in the MPL can be observed in Fig. 4(a), and the pore size of approximately 30μm thick MPL is much smaller than that of the GDL (Fig. 4(b)). The images clearly show the microstructure of the MPL, with mean pore diameter smaller than 0.5μm as reported previously [13].

Figures 4(c) - (f) are images after operating the cell. Figures 4(c) and (d) are typical images from inside the MPL with Cases A and B respectively, with the ice distributions clearly different for the two operating conditions. With Case A in Fig. 4(c), operation at 35ºC, there is no ice observed inside the MPL and the original porous structure can be observed. If the produced water passes through the MPL in the liquid phase in Case A, the liquid water would remain inside the hydrophobic MPL to be observed as ice in Fig. 4(c). The absence of ice formations suggests that the produced water passes through the MPL in vapor form at ordinary operating temperatures, above 35ºC. Existence of cracks in the MPL may play an important role for water transport, but no cracks were found in our number of observation images. In Case B, with the cell operation temperature at 5ºC (Fig. 4(d)), the porous structure of the MPL is filled with ice. It may be assumed that when the cell temperature is low, liquid water accumulates in the pores of the MPL. These results agree with the analysis by Owejan et al. [7], which is based on the vapor flux due to the saturation pressure gradient corresponding to the temperature gradient for heat conduction through the MPL. Calculating the vapor transport rate with standard MPL material properties, all of the produced water can be transported in the vapor phase through MPL when the temperature is higher than the critical value around 35ºC.

Figures 4(e) and (f) are images of the MPL/CL interface with ice layers in Case A and Case B, respectively, although depending on locations there was no ice between the layers. The ice distributions at the MPL/CL interface are different due to the different cell operating temperatures. In Case A, a 2 to 3μm thick ice layer can be observed at the MPL/CL interface (Fig. 4(e)). At the lower operating temperature in Case B, there is a thicker formation of ice, about 8μm thick, between the MPL and the catalyst layer (Fig. 4(f)). In Case B, the locations of the images were identified: Figs. 4(d) and (f) are from under the land and the channel respectively. The ice distribution in Fig. 4(d) shows that the porous structure of the MPL is

filled with ice under the land. At the MPL/CL interface under the channel there is a sizeable formation of ice, while it appears that there is no ice in the MPL under the channel (Fig. 4(f)).

As above, it is demonstrated that the freezing method can be used to elucidate details of the approximate water distribution resulting from the operation of a PEFC.

Conclusions

The paper analyzes water transport phenomena in the vicinity of the cathode MPL using a freezing method where the liquid water in the cell was frozen and cross sectional images were observed with cryo-SEM. The results of the experiments indicate that the produced water passes through the MPL as vapor under ordinary operating temperatures, above 35ºC, while liquid water accumulates in the MPL at the low operating temperature of 5ºC. The observations also show that the liquid water tends to accumulate in the interface between the MPL and catalyst layer under the channels and in the pores of the MPL under lands. The paper demonstrates the usefulness of the freezing method for the water transport investigations in PEFCs.

Acknowledgment

The authors thank Y. Takeya and K. Okada (undergraduate students of Hokkaido University) for their help in the experiments and in the cryo-SEM observations.

References

[1] U. Pasaogullari, C. Y. Wang, K. S. Chen, J. Electrochem. Soc. 152 (2005) A1574.
[2] T. Tanuma, J. Electrochem. Soc. 157 (2010) B1809.
[3] S. Kim and M. M. Mench, J. Electrochem. Soc. 156 (2009) B353.
[4] A. Z. Weber and M. A. Hickner, Electrochim. Acta 53 (2008) 7668.
[5] A. Z. Weber and J. Newman, J. Electrochem. Soc. 152 (2005) A677.
[6] J.T. Gostick, M.A. Ioannidis, M.W. Fowler, M.D. Pritzker, Electrochem. Commun. 11 (2009) 576.
[7] J. P. Owejan, J. E. Owejan, W. Gu, T. Trabold, T. Tighe, M. Mathias, J. Electrochem. Soc. 157 (2010) B1456.
[8] F. E. Hizir, S. O. Ural, E. C. Kumbur, M. M. Mench, J. Power Sources 195 (2010) 3463
[9] P. Boillat, D. Kramer, B. C. Seyfang, G. Frei, E. Lehmann, G. G. Scherer, A. Wokaun, Y. Ichikawa, Y. Tasaki, K. Shinohara, Electrochem. Commun. 10 (2008) 546.
[10] J. Lee, J. Hinebaugh, A. Bazylak, J. Power Sources 227 (2013) 123.
[11] T. Sasabe, P. Deevanhxay, S. Tsushima, S. Hirai, Electrochem. Commun. 13 (2011) 638.
[12] K. S. S. Naing, Y. Tabe, T. Chikahisa, J. Power Sources 196 (2011) 2584.
[13] J. H. Nam, K. Lee, G. Hwang, C. Kim, J. Heat and Mass Transfer 52 (2009) 2779.

Fig. 1. Procedures of the freezing method.
Fig. 2. Cryo-SEM images of ice in the cell.
Fig. 3. Changes in the cell voltage and resistance for Cases A and B.
Fig. 4. Cryo-SEM images of the vicinity of the cathode MPL.

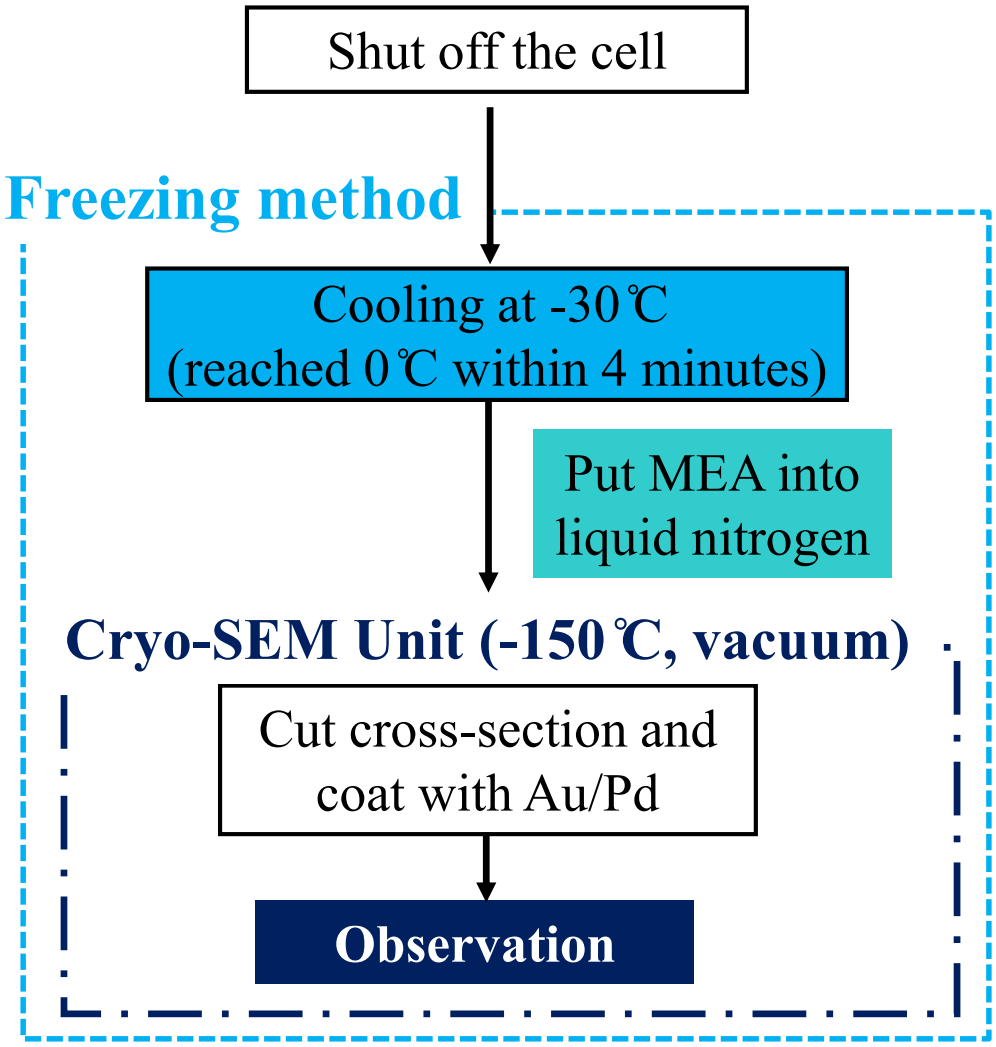

Fig. 1. Procedures of the freezing method.

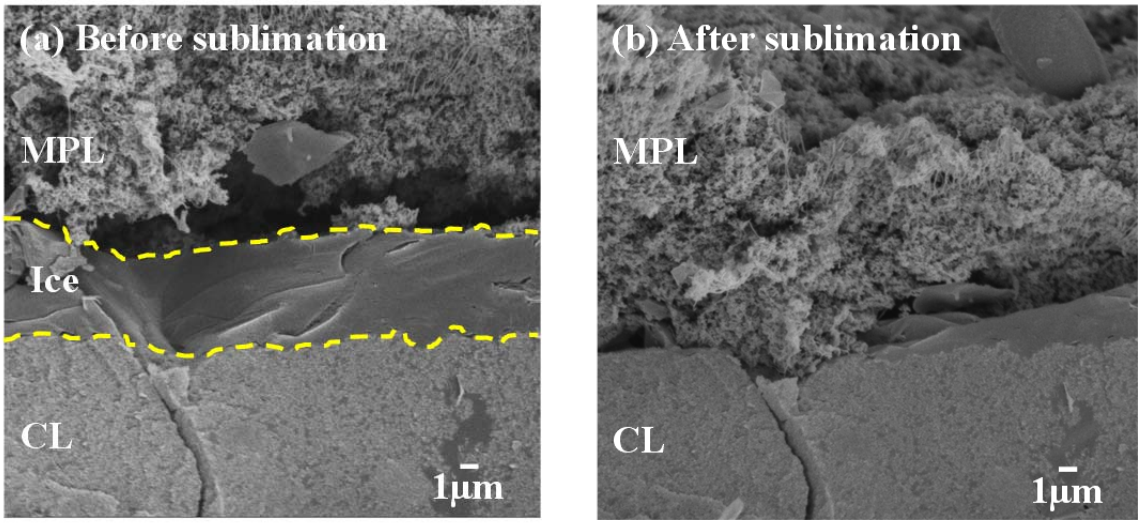

Fig. 2. Cryo-SEM images of ice in the cell.

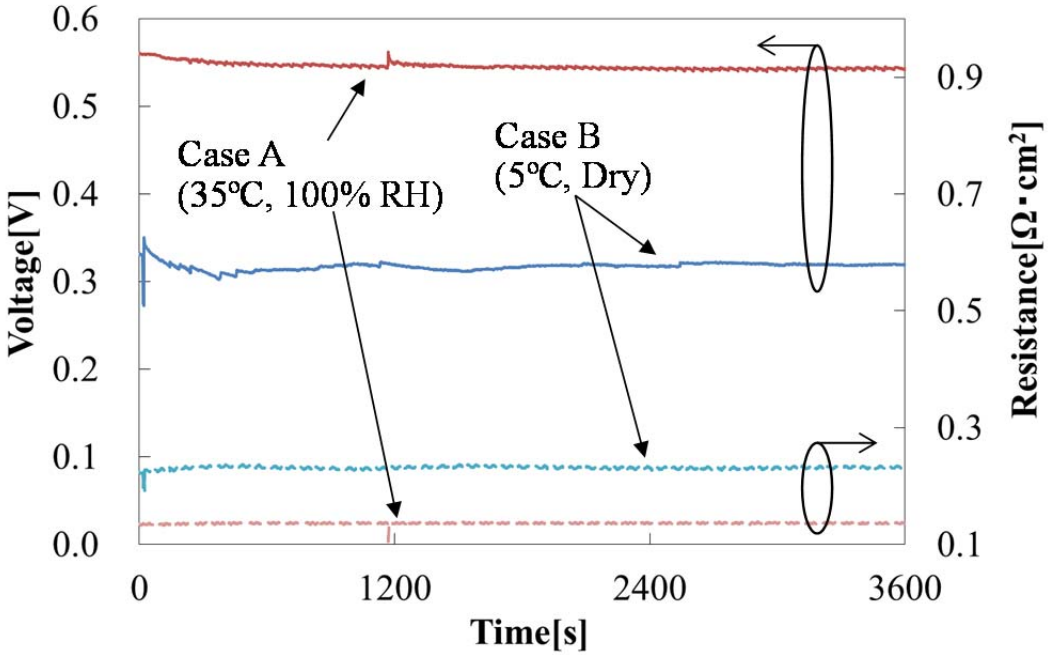

Fig. 3. Changes in the cell voltage and resistance for Cases A and B.

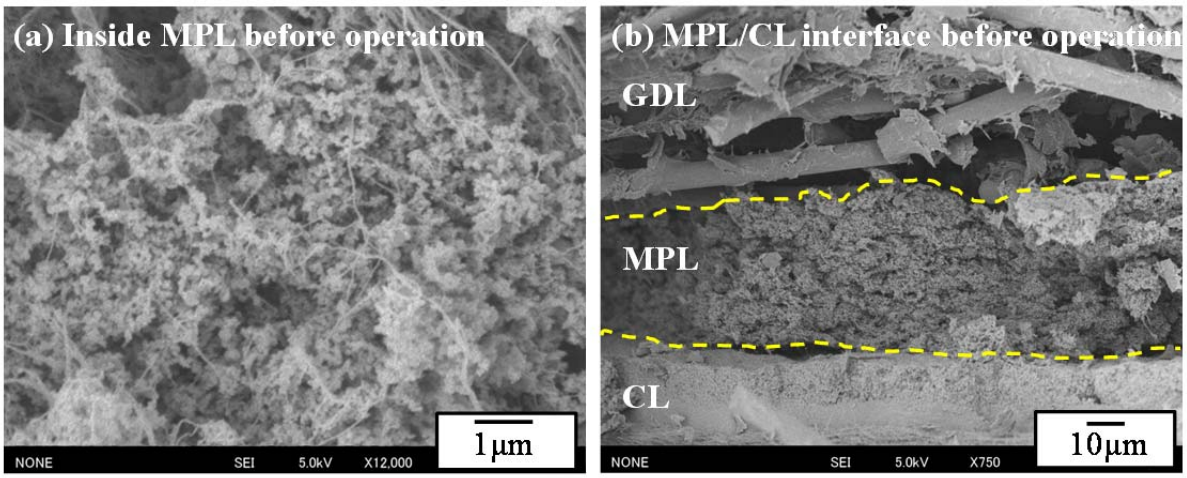

Fig. 4. Cryo-SEM images of the vicinity of the cathode MPL.

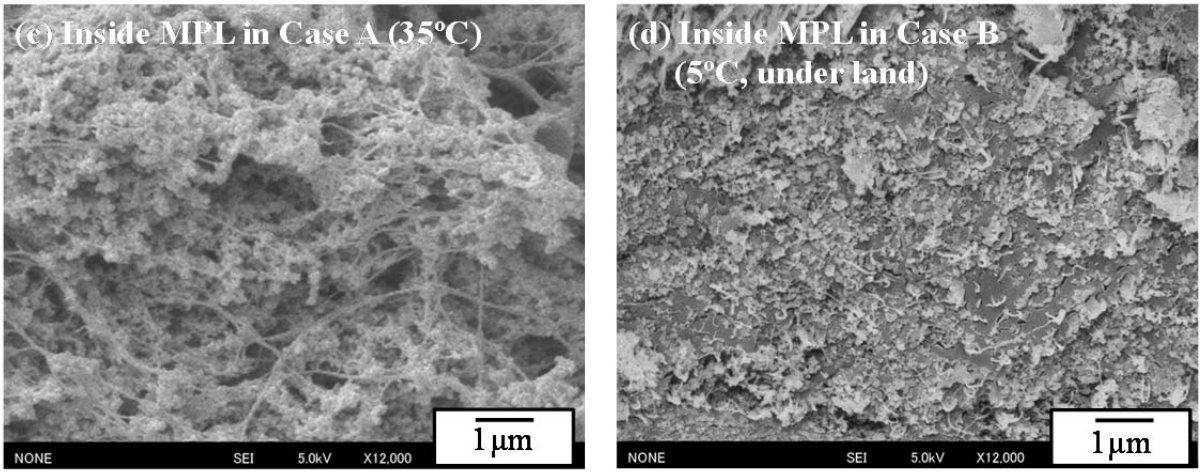

Fig. 4. Cryo-SEM images of the vicinity of the cathode MPL.

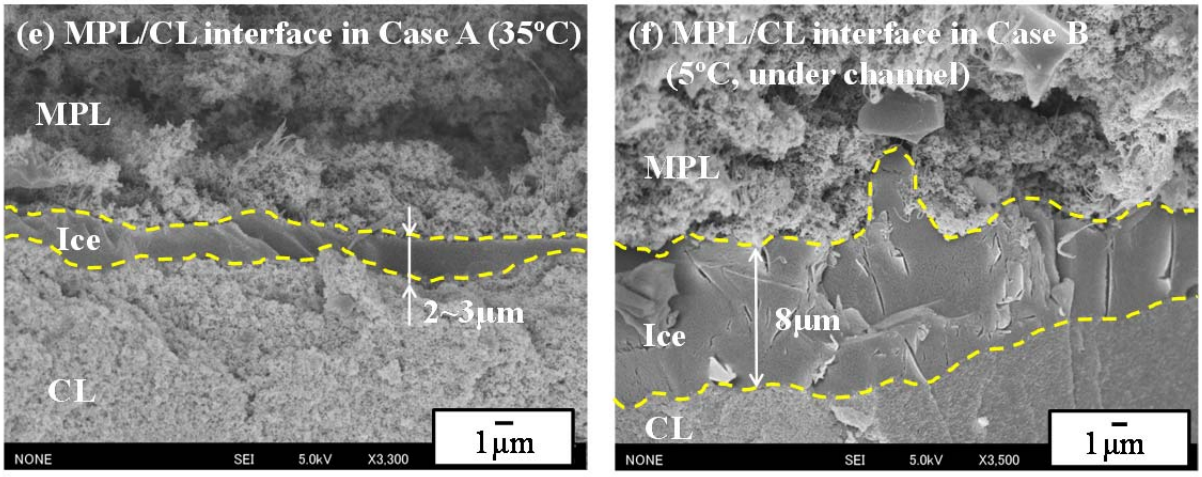

Fig. 4. Cryo-SEM images of the vicinity of the cathode MPL.